Garnierite characterisation for open data bases for nickel laterite exploration

Nicolas Maubec, Pierre Gilles Blaineau, Cédric Duée, Anthony Da Silva Alves, Xavier Bourrat, Guillaume Wille
BRGM, 3 avenue Claude Guillemin, BP 36009, 45060 Orléans Cédex, France

Beate Orberger
GEOPS, Université Paris Saclay, Bât 504, 91405 Orsay Cedex, France
CATURA Geoprojects, 2 rue Marie Davy, 75014 Paris, France

Monique Le Guen
ERAMET IDEA, 1 avenue Albert Einstein, 78190 Trappes, France

Cristina Villanova-de-Benavent
Departament de Mineralogia, Petrologia i Geologia Aplicada, Facultat de Geologia, Universitat de Barcelona (UB), C/Marti i Franquès, s/n -08028, Barcelona, Spain

Abstract. In order to develop a mineralogical and chemical database, which will be associated with an on-line-on mine instrument, for nickel mining exploration, several garnierite samples were studied in laboratory. The collected samples are Ni-bearing laterites from New Caledonia and Dominican Republic and are mainly composed of serpentine-like and/or talc-like and/or sepiolite-like phase. These three types of phases are clearly differentiated by X-ray diffractometry (XRD). The presence of Ni within the crystallographic structure of these phases can be observed from the infrared or Raman spectra, where the effect of Mg/Ni substitutions causes shifts in some bands. The relative intensity of these bands can be correlated with the Ni content. These different parameters are a reliable indicator to define the nature of garnierite and to have an indication on the Ni content.

1 Introduction

On-line–real time drill core scanner may comprise sensors such as Red – Green – Blue (RGB) cameras, profilometer, X-Ray Fluorescence (XRF) and hyperspectral cameras, X-Ray diffractometer (XRD) and Raman spectrometer. The analyses are performed on-line, and data interpretation relies on data bases with accurate and precise analyses on reference samples. Some data bases are available via the USGS Spectral Library (Kokaly et al. 2017) or CSIRO Mineral Spectral Libraries (Laukamp et al. 2019). However, these databases are not necessarily suitable for mining industries that need custom databases tailored to their specific ore types.

Nickel laterites are the most important Nickel source for the industries. It represents 60-70% of the total nickel resource in the world (Dalvi et al. 2004). They are complex soils with heterogeneous grain sizes (nanometric minerals to centimetric large aggregates or concretions). Nickel is present in several types of phyllosilicates (serpentine, chlorite, clay minerals and talc), which are sometimes agglomerated to garnierite (Gleeson et al. 2004; Soler et al. 2008).

The SOLSA project develops a coupled expert system comprising a sonic drill module, a core-scanner including RGB camera, profilometer, a XRF spectrometer and VNIR and SWIR cameras, and a XRD-XRF-Raman-benchtop system. The core scanner will define regions of interests (economic or for processing designs), while combined XRD-XRF-Raman will only analyze the regions of interest.

In this paper, we present detailed analyses on garnierites from different laterite sites in the world with the aim to calibrate and evaluate optical, chemical and mineralogical characteristics of the garnierite varieties, and to quickly categorize it for mining and processing purposes. All analyses will be entered in the Open Data Bases developed in the frame of the SOLSA H2020 project (www.solsamining.eu), and available for mining companies.

2 Sample material

A set of representative Garnierites of different facies and mineralogies from New Caledonia and the Dominican Republic were used for this work (Fig.1).

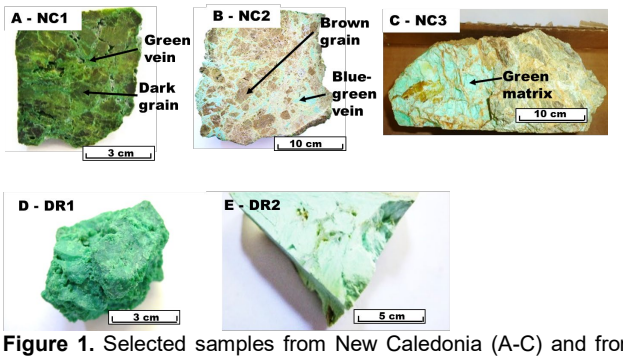

Figure 1. Selected samples from New Caledonia (A-C) and from Dominican Republic (D-E)

Three samples, referenced NC1 to NC3, are from New Caledonia (Fig. 1A-C). Samples NC1 and NC2 are characterized by the occurrence of green veins (dark green for NC1, blue-green for NC2) surrounding darker

grains. The third sample (NC3) does not have veins but has a blue-green matrix associated with brown regions. Samples DR1 and DR2 are from the Falcondo deposit in Dominican Republic (Fig. 1D-E). Sample DR1 features green blocs within bulky lighter grains while sample DR2 displays light blue fibbers.

3 Methodology

3.1 Sample preparation

The samples were analyzed by electron probe micro-analysis (EPMA), XRD, Fourier Transform, Infrared (FTIR) and micro-Raman spectroscopies for their chemical and mineralogical characterizations. Raman spectroscopy and EPMA were performed on polished thin sections, representing the different areas of interest (garnierites and associated phases).The XRD and FTIR analyses were carried out on powders. Because of the heterogeneity of the samples, it was decided to hand-pick a few tens of milligrams from different areas of each sample, in order to obtain "pure" phases. The targeted areas were greenish veins and matrices, as well as dark grains. The powder samples were ground in an agate mortar and sieved to 63 µm.

3.2. Analytical methods

Quantitative electron probe microanalyses were performed with a CAMECA SX FIVE electron microprobe equipped with five vertical spectrometers. The analyses were performed on carbon-coated (20 – 30 nm) polished thin sections using a 15 kV acceleration voltage, 20 nA probe current and 1-2 µm spot size. For each sample, the chemical composition was obtained from about ten measurement points.

The XRD analyses were performed on randomly oriented samples. For each sample, tens milligrams of powders were set on a zero-background sample holder. The diffractograms were acquired with a Bruker D8 Advance DA VINCI diffractometer equipped of a CuKα source (λ = 1.5406 Å), operating at 40kV and 40mA, and a LYNXEYE XE 1D detector with a 3.3° opening. The XRD patterns were measured in continuous scan mode over the 4-75°2θ range with a step size and a measuring time of 0.03°2θ and 576 seconds per step, respectively.

FTIR spectra were obtained using a Bruker Equinox 55 FTIR spectrometer, equipped with a middle-infrared (MIR) source and a KBr beam splitter. For each sample, 30 scans in the 4000-400 cm^{-1} spectral range were recorded with a resolution of 4 cm^{-1}. The analyses were carried out on pellets discs consisting of a mixture of 0.5 mg of sample and 150 mg of KBr. Before being analyzed, the pellets were stored at 60°C to minimize the absorption of water on KBr and on the sample.

Raman measurements were performed with a Renishaw InVIA Reflex microspectrometer coupled to a DMLM Leica microscope. Three different lasers were used (λ0 = 514.5 nm; 633 nm and 785 nm). The analyses were carried out using thin-sections observed with a x100 objective (NA = 0.90) or x50 objective and exposed to a laser beam with a power of around 1 mW at the sample surface. The Raman spectrometer was operated using continuous scanning mode with large spectral windows from 100 to 4000 cm^{-1}. Acquisition times (generally over 10 seconds) and accumulations of spectra vary depending for instance on the mineral type.

4 Results

The chemical compositions of the different samples, obtained by EPMA, are presented in Table 1. Each sample is mainly composed of Si, Mg, Ni. These are the main elements of the silicate phases found in garnierites. Only NC1_dark grain and NC2_brown grain contains some percents of Fe.

From a mineralogical point of view, the clay minerals found in garnierites form solid solutions by substituting Mg with Ni. The Ni(Ni+Mg) ratio gives an indication of these substitutions. In the present study, this ratio varies from 14% to 97% and indicates a fairly wide diversity in composition from one sample to another. It is also interesting to note that for samples that come from the same piece, such as NC1 and NC2, the Ni content is much higher in the veins than in the grains.

Table 1. Average composition of samples measured EPMA

	Wt %	SiO_2	Al_2O_3	MgO	Cr_2O_3	MnO	FeO	CoO	NiO	Total	Ni/(Ni+Mg) (%)
NC1_dark grain_1	Av	40.97	0.09	32.73	0.02	0.05	2.41	0.11	9.34	85.73	27
	σ	0.72	0.02	1.28	0.04	0.04	0.18	0.02	1.37	1.50	
NC1_green vein_2	Av	33.06	0.02	2.21	0.03	0.01	0.10	0.56	50.84	86.91	97
	σ	1.22	0.02	1.07	0.02	0.03	0.13	0.21	2.92	2.60	
NC2_Brown grain_3	Av	37.77	0.01	34.62	0.00	0.05	5.62	0.03	4.17	82.32	14
	σ	1.16	0.01	2.26	0.00	0.05	1.33	0.03	1.54	2.76	
NC2_green vein_4	Av	50.73	0.04	23.11	0.00	0.03	0.14	0.01	8.91	83.06	33
	σ	2.58	0.02	2.59	0.01	0.03	0.24	0.01	1.50	3.78	
NC3_green matrix_5	Av	54.53	0.01	19.86	0.00	0.00	0.00	0.01	18.97	93.52	55
	σ	1.69	0.01	1.14	0.01	0.00	0.00	0.02	1.70	0.73	
DR1_green matrix_6	Av	40.93	0.01	5.61	0.00	0.01	0.11	0.02	41.68	88.52	91
	σ	1.49	0.02	0.76	0.01	0.02	0.09	0.04	1.20	0.85	
DR2_green matrix_7	Av	47.15	0.03	16.43	0.00	0.02	0.04	0.00	23.14	86.95	65
	σ	2.85	0.02	2.88	0.00	0.02	0.08	0.00	4.79	1.62	

Mineralogical analyses obtained by XRD allow identifying the main mineralogical families featured into garnierite. These families are often called according to their basal d_{001} reflection: "serpentine-like" phase (7Å), "talc-like" phase (10Å) as well as "sepiolite-like" phase (12 Å) (Villanova-de-Benavent et al. 2014). In the present study, the three families are detected by peaks located at 7.3 Å, 10.2 Å and 12.1 Å (Figure 2). The two powders obtained from NC1 sample are mainly composed of serpentine-like minerals. Between the two diffractograms (NC1_dark grain and NC1_green vein), only a difference in peak width is visible. This difference is probably related to the significant presence of Ni into the veins in contrast to the grain.

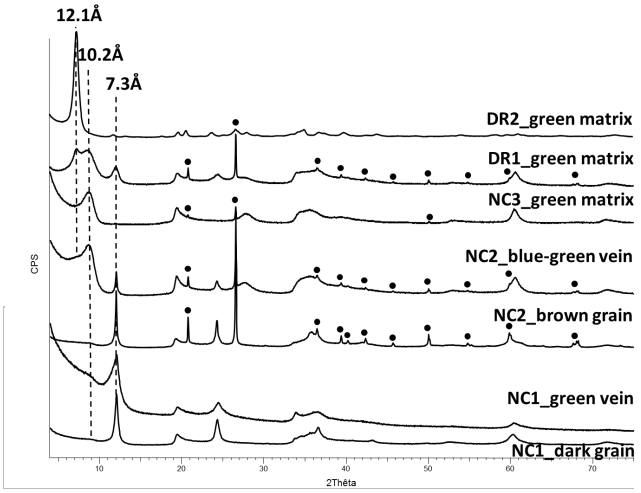

Figure 2. X-ray diffractograms of selected samples, with basal (interlayer) distances of serpentine-like, talc-like and sepiolite-like phases at 7.3Å, 10.2Å and 12.1Å, respectively. Black circles correspond to quartz peaks.

The two samples taken from the NC2 sample have a different mineralogical composition. NC2_brown grain is mainly composed of serpentine and quartz, while NC2_blue green vein is a mixture of talc-like, serpentine-like phase and quartz and probably also sepiolite-like phase. The NC3_green matrix sample is a relatively pure sample of talc-like phase with only traces of quartz detected. As for the NC2_blue green vein sample, the characteristic peaks of talc-like phase are broad. The DR1_green matrix sample has a complex composition consisting of the three types of clay minerals (serpentine-like, talc-like and sepiolite-like) as well as quartz. According to EPMA analyses, Ni is very abundant in relation to Mg and can be located within the crystallographic structures of the three clay phases. The DR2_green matrix is a pure sample of sepiolite-like phase characterized by a main peak at 12.1 Å.

The spectra obtained by FTIR, on the spectra ranges between 3000-3800 cm^{-1} and 500-1200 cm^{-1} (Fig. 3).

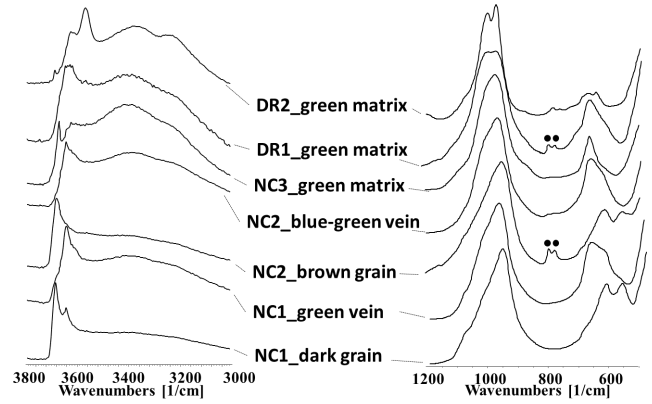

Figure 3. Infrared spectra of selected samples, in the 3000-3800 cm^{-1} and 500-1200 cm^{-1} spectral ranges. Black circles correspond to quartz bands.

Each spectrum shows three series of absorption bands; one between 500 and 700 cm^{-1}, the second between 900 and 1100 cm^{-1} and the third between 3500 and 3700 cm^{-1}. Between 500 and 700 cm^{-1}, the results show that there are similarities between the samples NC1_dark grain and NC2_brown grain. For these two samples, there are two absorption bands located around 550 cm^{-1} and 605 cm^{-1}. The similarity between these two samples is consistent with the previous data indicating that they are Mg-rich serpentines. On the other hand, the comparison with a Ni-rich serpentine, such as that present in the NC1_green vein sample, shows a difference in the position of these bands. For this sample, the bands are around 660 cm^{-1} and 610 cm^{-1}. In the case of a sample rich in talc-like phase (NC3_green matrix), there is a characteristic band centered around 665 cm^{-1} with a shoulder towards 610 cm^{-1}. These are the same positions as those observed for the Ni serpentine. This similarity is certainly related to an environment around Ni that is comparable between the two clay structures. Compared to the other samples, sepiolite-like phase (DR2_green matrix) is characterized by two bands of low intensities at 643 cm^{-1} and 670 cm^{-1}. For samples consisting of phase mixtures, the bands are relatively broad and poorly resolved. They consist of the association of the different absorption bands that characterize the different clay minerals. In the 900-1100 cm^{-1}, the spectra have very similar characteristic. Except for sepiolite-like phase, the samples are characterized by an asymmetric band with a maximum located between 950 and 975 cm^{-1}, and a shoulder around 1080 cm^{-1}. In this absorption domain, it is the vibration modes of the SiO_4 tetrahedra that are at stake (Suarez and Garcia-Romero 2006). Only sepiolite is distinguished by the presence of two well-defined bands at 974 cm^{-1} and 1002 cm^{-1}. These bands are perceptible in DR1_green matrix which also contains sepiolite. The 3500-3800 cm^{-1} range is characteristic of the vibrations of hydroxyl groups associated with R-(O,OH) octahedra (where R = Mg or Ni) (Baron and Petit 2016; Suarez and Garcia-Romero 2006). The position of the bands will depend on the Mg/Ni substitutions. This is particularly the case when comparing the spectra between the Mg-rich serpentines (NC1_dark grain or NC2_brown grain) and the Ni-rich serpentine (NC1_green vein); the bands present at 3687 cm^{-1} and 3646 cm^{-1} shift towards lower frequencies in the presence of Ni (3646 cm^{-1} and 3608 cm^{-1}, respectively). In the talc-like sample (NC3_green matrix), there are similarly located bands. The difference with serpentines comes from the presence of very broad bands between 3100 and 3500 cm^{-1} attributed to the vibrations of the water molecules present in the structure (Gerard and Herbillon 1983). The sepiolite-like sample (DR2_green matrix) differs from the other samples by the presence of two well-defined bands at 3628 cm^{-1} and 3569 cm^{-1} in addition to broad bands due to water molecules.

In addition to FTIR analyses, Raman spectroscopy makes it possible to differentiate between the different types of clay minerals (Figure 4).

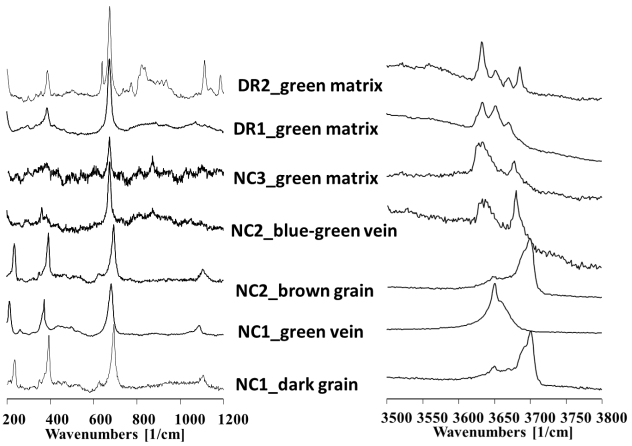

Figure 4. Raman spectra of selected samples, in the 200-1200 cm^{-1} and 3500-3800 cm^{-1} spectral ranges.

Serpentine-like sample (NC1_dark grain and NC2_brown grain) are characterized by four main bands in the range 200 - 1200 cm^{-1}, located around 230 cm^{-1}, 390 cm^{-1}, 690 cm^{-1} and 1105 cm^{-1}, as well as several bands between 3650 and 3700 cm^{-1}. In the presence of a high Ni content (in the case of the NC1_green vein sample), all the bands are shifted towards lower wavenumbers compared to those present in Mg-rich serpentines (NC1_dark grain and NC2_brown grain). Compared to serpentines, talc-rich samples (NC2_blue green vein and NC3_green matrix) are marked with a main band at 675 cm^{-1}. Bands with low intensity around 380 cm^{-1} and 870 cm^{-1} may also be visible. In the 3500 - 3800 cm^{-1} range, the two samples are characterized by a well resolved band at 3678 cm^{-1} accompanied by a broad band centered at 3632 cm^{-1}. The only visible difference between these two samples is the intensity ratio between these two bands (I_{3632} / I_{3678}). This ratio is higher for the sample with a higher Ni content, namely NC3_green matrix (Table 1). Sepiolite minerals (DR2_green matrix) are clearly distinguished from other samples by the presence of four well-defined bands located at 3633 cm^{-1}, 3651 cm^{-1}, 3669 cm^{-1} and 3686 cm^{-1}. Most of these bands are found in the DR1_green matrix sample but with different relative intensities.

4 Discussion and conclusions

A set of Ni-bearing laterites samples from New Caledonia and the Dominican Republic representative of the diversity of Ni-bearing clay minerals has been characterized using different analytical techniques (EPMA, XRD, FTIR and Raman micro spectroscopy).

The garnierites characterized in this study are composed of either serpentine-like, and/or talc-like and/or sepiolite-like phase(s). These three types of clay phases (serpentine-like, talc-like and sepiolite-like) can form series of solid solutions by substituting Mg for Ni (Gleeson et al. 2004). The presence of nickel is first visible to the naked eye where the areas enriched in this element tend to be green or blue green. Then, in analytical point of view, the effect of the substitutions of Mg by Ni generates a structural disorder which results in the broadening of diffraction peaks (Baron and Petit 2016). This is the case for Ni-rich serpentine (NC1_green vein) and talc-like phase where Ni is important. Then the presence of Ni within the crystallographic structures induces differences (peak shift) on the spectra obtained by FTIR and Raman spectroscopy. The observed shifts are due to the nature of the cations (Mg^{2+} or Ni^{2+}) which will have an influence both on the environment of the SiO_4 tetrahedra and on the properties (lengths, forces) of the R-O,OH bonds, where R = Mg or Ni (Baron and Petit 2016; Petriglieri et al. 2015).

All these data are important because they are indicators to define the nature of garnierite and to have an indication on the presence of Ni into the samples. These data are entered into the SOLSA Open data bases, which will be online by the end of the SOLSA project 2/202 and will be able to assist mining and metallurgical companies in exploration and mining exploitation.

Acknowledgements

This study received grants from the EU H2020 project SOLSA N°689868. Samples were provided by ERAMET, BRGM and University of Barcelona.

References

Baron F, Petit S (2016) Interpretation of the infrared spectra of the lizardite-nepouite series in the near- and mid-infrared range. American Mineralogist 101:423-430

Dalvi AD, Bacon WG, Osborne RC (2004) The past and the future of nickel laterites. PDAC 2004 International Convention, Trade Show and Investors Exchange, Canada, 1-27

Gerard P, Herbillon AJ (1983) Infrared studies of Ni-bearing clay minerals of the kerolite-pimelite series. Clays and Clay Minerals 31 : 143-151

Gleeson SA, Herrington RJ, Durango J, Velasquez CA, Koll G (2004) The mineralogy ang geochemistry of the Cerro Matoso SA Ni laterite deposit, Montelibano, Colombia. Economic Geology 99: 1197-1213

Kokaly RF, Clark RN, Swayze GA, Livo KE, Hoefen TM, Pearson NC, Wise RA, Benzel WM, Lowers HA, Driscoll RL, Klein AJ (2017) USGS Spectral Library Version 7. US Geological Survey Data Series 1035, 68 p.

Laukamp C, Lau I, Warren P (2019) CSIRO Mineral Spectral Libraries. CSIRO Mineral Resources https://mineralspectrallibraries.csiro.au/Home/Samples

Petriglieri JR, Salvioli-Mariani E, Mantovani L, Tribaudino M, Lottici PP, Laporte-Magoni C, Bersani D (2015) Micro-Raman mapping of the polymorphs of serpentine. Journal of raman spectroscopy 46 : 953-958

Soler JM, Carma J, Gali S, Melendez W, Ramirez A, Estanga J (2008) Composition and dissolution kinetics of garnierite from the Loma de Hierro Ni-laterite deposit, Venezuela. Chemical Geology, 249, 191-202

Suarez M, Garcia-Romero E (2006) FTIR spectroscopic study of palygorskite: influence of the composition of the octahedral sheet. Applied Clay Science 31: 154-163

Villanova-de-Benavent C, Proenza JA, Gali S, Garcia-Casco A, Tauler E, Lewis JF, Longo F (2014) Garnierites and garnierites: Textures, mineralogy and geochemistry of garnierites in the Falcondo Ni-laterite deposit, Dominican Republic. Ore Geology Reviews 58: 91-109